Fermilab-pub-95/101-E

Measurement of the $WW\gamma$ gauge boson couplings in $p\bar{p}$ Collisions at $\sqrt{s} = 1.8$ TeV

S. Abachi,[12] B. Abbott,[33] M. Abolins,[23] B.S. Acharya,[40] I. Adam,[10] D.L. Adams,[34] M. Adams,[15] S. Ahn,[12] H. Aihara,[20] J. Alitti,[36] G. Álvarez,[16] G.A. Alves,[8] E. Amidi,[27] N. Amos,[22] E.W. Anderson,[17] S.H. Aronson,[3] R. Astur,[38] R.E. Avery,[29] A. Baden,[21] V. Balamurali,[30] J. Balderston,[14] B. Baldin,[12] J. Bantly,[4] J.F. Bartlett,[12] K. Bazizi,[7] J. Bendich,[20] S.B. Beri,[31] I. Bertram,[34] V.A. Bezzubov,[32] P.C. Bhat,[12] V. Bhatnagar,[31] M. Bhattacharjee,[11] A. Bischoff,[7] N. Biswas,[30] G. Blazey,[12] S. Blessing,[13] P. Bloom,[5] A. Boehnlein,[12] N.I. Bojko,[32] F. Borcherding,[12] J. Borders,[35] C. Boswell,[7] A. Brandt,[12] R. Brock,[23] A. Bross,[12] D. Buchholz,[29] V.S. Burtovoi,[32] J.M. Butler,[12] D. Casey,[35] H. Castilla-Valdez,[9] D. Chakraborty,[38] S.-M. Chang,[27] S.V. Chekulaev,[32] L.-P. Chen,[20] W. Chen,[38] L. Chevalier,[36] S. Chopra,[31] B.C. Choudhary,[7] J.H. Christenson,[12] M. Chung,[15] D. Claes,[38] A.R. Clark,[20] W.G. Cobau,[21] J. Cochran,[7] W.E. Cooper,[12] C. Cretsinger,[35] D. Cullen-Vidal,[4] M.A.C. Cummings,[14] D. Cutts,[4] O.I. Dahl,[20] K. De,[41] M. Demarteau,[12] R. Demina,[27] K. Denisenko,[12] N. Denisenko,[12] D. Denisov,[12] S.P. Denisov,[32] W. Dharmaratna,[13] H.T. Diehl,[12] M. Diesburg,[12] G. Di Loreto,[23] R. Dixon,[12] P. Draper,[41] J. Drinkard,[6] Y. Ducros,[36] S.R. Dugad,[40] S. Durston-Johnson,[35] D. Edmunds,[23] J. Ellison,[7] V.D. Elvira,[12,‡] R. Engelmann,[38] S. Eno,[21] G. Eppley,[34] P. Ermolov,[24] O.V. Eroshin,[32] V.N. Evdokimov,[32] S. Fahey,[23] T. Fahland,[4] M. Fatyga,[3] M.K. Fatyga,[35] J. Featherly,[3] S. Feher,[38] D. Fein,[2] T. Ferbel,[35] G. Finocchiaro,[38] H.E. Fisk,[12] Yu. Fisyak,[24] E. Flattum,[23] G.E. Forden,[2] M. Fortner,[28] K.C. Frame,[23] P. Franzini,[10] S. Fuess,[12] A.N. Galjaev,[32] E. Gallas,[41] C.S. Gao,[12,*] S. Gao,[12,*] T.L. Geld,[23] R.J. Genik II,[23] K. Genser,[12] C.E. Gerber,[12,§] B. Gibbard,[3] V. Glebov,[35] S. Glenn,[5] B. Gobbi,[29] M. Goforth,[13] A. Goldschmidt,[20] B. Gómez,[1] P.I. Goncharov,[32] H. Gordon,[3] L.T. Goss,[42] N. Graf,[3] P.D. Grannis,[38] D.R. Green,[12] J. Green,[28] H. Greenlee,[12] G. Griffin,[6] N. Grossman,[12]

P. Grudberg,[20] S. Grünendahl,[35] W. Gu,[12,*] J.A. Guida,[38] J.M. Guida,[3] W. Guryn,[3] S.N. Gurzhiev,[32] Y.E. Gutnikov,[32] N.J. Hadley,[21] H. Haggerty,[12] S. Hagopian,[13] V. Hagopian,[13] K.S. Hahn,[35] R.E. Hall,[6] S. Hansen,[12] R. Hatcher,[23] J.M. Hauptman,[17] D. Hedin,[28] A.P. Heinson,[7] U. Heintz,[12] R. Hernández-Montoya,[9] T. Heuring,[13] R. Hirosky,[13] J.D. Hobbs,[12] B. Hoeneisen,[1,¶] J.S. Hoftun,[4] F. Hsieh,[22] Ting Hu,[38] Tong Hu,[16] T. Huehn,[7] S. Igarashi,[12] A.S. Ito,[12] E. James,[2] J. Jaques,[30] S.A. Jerger,[23] J.Z.-Y. Jiang,[38] T. Joffe-Minor,[29] H. Johari,[27] K. Johns,[2] M. Johnson,[12] H. Johnstad,[39] A. Jonckheere,[12] M. Jones,[14] H. Jöstlein,[12] S.Y. Jun,[29] C.K. Jung,[38] S. Kahn,[3] J.S. Kang,[18] R. Kehoe,[30] M.L. Kelly,[30] A. Kernan,[7] L. Kerth,[20] C.L. Kim,[18] S.K. Kim,[37] A. Klatchko,[13] B. Klima,[12] B.I. Klochkov,[32] C. Klopfenstein,[38] V.I. Klyukhin,[32] V.I. Kochetkov,[32] J.M. Kohli,[31] D. Koltick,[33] A.V. Kostritskiy,[32] J. Kotcher,[3] J. Kourlas,[26] A.V. Kozelov,[32] E.A. Kozlovski,[32] M.R. Krishnaswamy,[40] S. Krzywdzinski,[12] S. Kunori,[21] S. Lami,[38] G. Landsberg,[12] R.E. Lanou,[4] J-F. Lebrat,[36] A. Leflat,[24] H. Li,[38] J. Li,[41] Y.K. Li,[29] Q.Z. Li-Demarteau,[12] J.G.R. Lima,[8] D. Lincoln,[22] S.L. Linn,[13] J. Linnemann,[23] R. Lipton,[12] Y.C. Liu,[29] F. Lobkowicz,[35] S.C. Loken,[20] S. Lökös,[38] L. Lueking,[12] A.L. Lyon,[21] A.K.A. Maciel,[8] R.J. Madaras,[20] R. Madden,[13] I.V. Mandrichenko,[32] Ph. Mangeot,[36] S. Mani,[5] B. Mansoulié,[36] H.S. Mao,[12,*] S. Margulies,[15] R. Markeloff,[28] L. Markosky,[2] T. Marshall,[16] M.I. Martin,[12] M. Marx,[38] B. May,[29] A.A. Mayorov,[32] R. McCarthy,[38] T. McKibben,[15] J. McKinley,[23] H.L. Melanson,[12] J.R.T. de Mello Neto,[8] K.W. Merritt,[12] H. Miettinen,[34] A. Milder,[2] A. Mincer,[26] J.M. de Miranda,[8] C.S. Mishra,[12] M. Mohammadi-Baarmand,[38] N. Mokhov,[12] N.K. Mondal,[40] H.E. Montgomery,[12] P. Mooney,[1] M. Mudan,[26] C. Murphy,[16] C.T. Murphy,[12] F. Nang,[4] M. Narain,[12] V.S. Narasimham,[40] A. Narayanan,[2] H.A. Neal,[22] J.P. Negret,[1] E. Neis,[22] P. Nemethy,[26] D. Nešić,[4] D. Norman,[42] L. Oesch,[22] V. Oguri,[8] E. Oltman,[20] N. Oshima,[12] D. Owen,[23] P. Padley,[34] M. Pang,[17] A. Para,[12] C.H. Park,[12] Y.M. Park,[19] R. Partridge,[4] N. Parua,[40] M. Paterno,[35] J. Perkins,[41] A. Peryshkin,[12] M. Peters,[14] H. Piekarz,[13] Y. Pischalnikov,[33] A. Pluquet,[36] V.M. Podstavkov,[32] B.G. Pope,[23] H.B. Prosper,[13] S. Protopopescu,[3] D. Pušeljić,[20] J. Qian,[22] P.Z. Quintas,[12] R. Raja,[12] S. Rajagopalan,[38] O. Ramirez,[15]

M.V.S. Rao,[40] P.A. Rapidis,[12] L. Rasmussen,[38] A.L. Read,[12] S. Reucroft,[27] M. Rijssenbeek,[38] T. Rockwell,[23] N.A. Roe,[20] P. Rubinov,[38] R. Ruchti,[30] S. Rusin,[24] J. Rutherfoord,[2] A. Santoro,[8] L. Sawyer,[41] R.D. Schamberger,[38] H. Schellman,[29] J. Sculli,[26] E. Shabalina,[24] C. Shaffer,[13] H.C. Shankar,[40] R.K. Shivpuri,[11] M. Shupe,[2] J.B. Singh,[31] V. Sirotenko,[28] W. Smart,[12] A. Smith,[2] R.P. Smith,[12] R. Snihur,[29] G.R. Snow,[25] S. Snyder,[38] J. Solomon,[15] P.M. Sood,[31] M. Sosebee,[41] M. Souza,[8] A.L. Spadafora,[20] R.W. Stephens,[41] M.L. Stevenson,[20] D. Stewart,[22] D.A. Stoianova,[32] D. Stoker,[6] K. Streets,[26] M. Strovink,[20] A. Taketani,[12] P. Tamburello,[21] J. Tarazi,[6] M. Tartaglia,[12] T.L. Taylor,[29] J. Teiger,[36] J. Thompson,[21] T.G. Trippe,[20] P.M. Tuts,[10] N. Varelas,[23] E.W. Varnes,[20] P.R.G. Virador,[20] D. Vititoe,[2] A.A. Volkov,[32] A.P. Vorobiev,[32] H.D. Wahl,[13] J. Wang,[12,*] L.Z. Wang,[12,*] J. Warchol,[30] M. Wayne,[30] H. Weerts,[23] W.A. Wenzel,[20] A. White,[41] J.T. White,[42] J.A. Wightman,[17] J. Wilcox,[27] S. Willis,[28] S.J. Wimpenny,[7] J.V.D. Wirjawan,[42] J. Womersley,[12] E. Won,[35] D.R. Wood,[12] H. Xu,[4] R. Yamada,[12] P. Yamin,[3] C. Yanagisawa,[38] J. Yang,[26] T. Yasuda,[27] P. Yepes,[34] C. Yoshikawa,[14] S. Youssef,[13] J. Yu,[35] Y. Yu,[37] Y. Zhang,[12,*] Y.H. Zhou,[12,*] Q. Zhu,[26] Y.S. Zhu,[12,*] Z.H. Zhu,[35] D. Zieminska,[16] A. Zieminski,[16] and A. Zylberstejn[36]

(DØ Collaboration)

[1] *Universidad de los Andes, Bogotá, Colombia*

[2] *University of Arizona, Tucson, Arizona 85721*

[3] *Brookhaven National Laboratory, Upton, New York 11973*

[4] *Brown University, Providence, Rhode Island 02912*

[5] *University of California, Davis, California 95616*

[6] *University of California, Irvine, California 92717*

[7] *University of California, Riverside, California 92521*

[8] *LAFEX, Centro Brasileiro de Pesquisas Físicas, Rio de Janeiro, Brazil*

[9] *CINVESTAV, Mexico City, Mexico*

[10] *Columbia University, New York, New York 10027*

[11] *Delhi University, Delhi, India 110007*

[12] *Fermi National Accelerator Laboratory, Batavia, Illinois 60510*

[13] *Florida State University, Tallahassee, Florida 32306*

[14] *University of Hawaii, Honolulu, Hawaii 96822*

[15] *University of Illinois at Chicago, Chicago, Illinois 60607*

[16] *Indiana University, Bloomington, Indiana 47405*

[17] *Iowa State University, Ames, Iowa 50011*

[18] *Korea University, Seoul, Korea*

[19] *Kyungsung University, Pusan, Korea*

[20] *Lawrence Berkeley Laboratory and University of California, Berkeley, California 94720*

[21] *University of Maryland, College Park, Maryland 20742*

[22] *University of Michigan, Ann Arbor, Michigan 48109*

[23] *Michigan State University, East Lansing, Michigan 48824*

[24] *Moscow State University, Moscow, Russia*

[25] *University of Nebraska, Lincoln, Nebraska 68588*

[26] *New York University, New York, New York 10003*

[27] *Northeastern University, Boston, Massachusetts 02115*

[28] *Northern Illinois University, DeKalb, Illinois 60115*

[29] *Northwestern University, Evanston, Illinois 60208*

[30] *University of Notre Dame, Notre Dame, Indiana 46556*

[31] *University of Panjab, Chandigarh 16-00-14, India*

[32] *Institute for High Energy Physics, 142-284 Protvino, Russia*

[33] *Purdue University, West Lafayette, Indiana 47907*

[34] *Rice University, Houston, Texas 77251*

[35] *University of Rochester, Rochester, New York 14627*

[36] *CEA, DAPNIA/Service de Physique des Particules, CE-SACLAY, France*

[37] *Seoul National University, Seoul, Korea*

[38] *State University of New York, Stony Brook, New York 11794*

[39] *SSC Laboratory, Dallas, Texas 75237*

[40] *Tata Institute of Fundamental Research, Colaba, Bombay 400005, India*

[41] *University of Texas, Arlington, Texas 76019*

[42] *Texas A&M University, College Station, Texas 77843*

(August 18, 2018)

Abstract

The $WW\gamma$ gauge boson couplings were measured using $p\bar{p} \to \ell\nu\gamma + X$ ($\ell = e, \mu$) events at $\sqrt{s} = 1.8$ TeV observed with the DØ detector at the Fermilab Tevatron Collider. The signal, obtained from the data corresponding to an integrated luminosity of 13.8 pb^{-1}, agrees well with the Standard Model prediction. A fit to the photon transverse energy spectrum yields limits at the 95% confidence level on the CP–conserving anomalous coupling parameters of $-1.6 < \Delta\kappa < 1.8$ ($\lambda = 0$) and $-0.6 < \lambda < 0.6$ ($\Delta\kappa = 0$).

Direct measurement of the $WW\gamma$ gauge boson couplings is possible through study of $W\gamma$ production in $p\bar{p}$ collisions at $\sqrt{s} = 1.8$ TeV. The most general effective Lagrangian [1], invariant under $U(1)_{EM}$, for the $WW\gamma$ interaction contains four coupling parameters, CP–conserving κ and λ, and CP–violating $\tilde{\kappa}$ and $\tilde{\lambda}$. The CP–conserving parameters are related to the magnetic dipole (μ_W) and electric quadrupole (Q_W^e) moments of the W boson, while the CP–violating parameters are related to the electric dipole (d_W) and the magnetic quadrupole (Q_W^m) moments: $\mu_W = (e/2m_W)(1+\kappa+\lambda)$, $Q_W^e = (-e/m_W^2)(\kappa-\lambda)$, $d_W = (e/2m_W)(\tilde{\kappa}+\tilde{\lambda})$, $Q_W^m = (-e/m_W^2)(\tilde{\kappa}-\tilde{\lambda})$ [2]. In the Standard Model (SM) the $WW\gamma$ couplings at the tree level are uniquely determined by the $SU(2)_L \otimes U(1)_Y$ gauge symmetry: $\kappa = 1$ ($\Delta\kappa \equiv \kappa - 1 = 0$), $\lambda = 0$, $\tilde{\kappa} = 0$, $\tilde{\lambda} = 0$. The direct and precise measurement of the $WW\gamma$ couplings is of interest since the existence of anomalous couplings, i.e. measured values different from the SM predictions, would indicate the presence of physics beyond the SM. A $WW\gamma$ interaction Lagrangian with constant, anomalous couplings violates unitarity at high energies, and, therefore, the coupling parameters must be modified to include form factors (e.g. $\Delta\kappa(\hat{s}) = \Delta\kappa/(1+\hat{s}/\Lambda^2)^n$, where $\hat{s}$ is the square of the invariant mass of the W and the photon, Λ is the form factor scale, and $n = 2$ for a dipole form factor) [3].

We present a measurement of the $WW\gamma$ couplings using $p\bar{p} \to \ell\nu\gamma + X$ ($\ell = e, \mu$) events observed with the DØ detector [4] during the 1992–1993 run of the Fermilab Tevatron Collider, corresponding to an integrated luminosity of 13.8 ± 0.7 pb^{-1}. These events contain the $W\gamma$ production process, $p\bar{p} \to W\gamma + X$ followed by $W \to \ell\nu$, and the radiative $W \to \ell\nu\gamma$ decay where the photon originates from bremsstrahlung of the charged lepton. Anomalous coupling parameters enhance the $W\gamma$ production with a large $\hat{s}$, and thereby result in an excess of events with high transverse energy, E_T, photons, well separated from the charged lepton. In the following, the electron and muon channels are referred to as $W(e\nu)\gamma$ and $W(\mu\nu)\gamma$, respectively.

The DØ calorimeter system consists of uranium–liquid argon sampling detectors in a central and two end cryostats, with a scintillator tile array in the inter-cryostat regions. The calorimeter [5] provides hermetic coverage for $|\eta| < 4.4$ with energy resolution of

$15\%/\sqrt{E(\mathrm{GeV})}$ for electrons and $50\%/\sqrt{E}$ for isolated pions, where η is the pseudorapidity defined as $\eta = -\ln(\tan(\theta/2))$, θ being the polar angle with respect to the beam axis. The calorimeter is read out in towers that subtend $\Delta\eta \times \Delta\phi = 0.1 \times 0.1$, ϕ being the azimuthal angle, and are segmented longitudinally into 4 electromagnetic (EM) and 4–5 hadronic layers. In the third EM layer, which typically contains 65% of the EM shower energy, the towers are subdivided transversely into $\Delta\eta \times \Delta\phi = 0.05 \times 0.05$. The central and forward drift chambers are used to identify charged tracks for $|\eta| < 3.2$. The muon system consists of magnetized iron toroids with one inner and two outer layers of drift tubes, providing coverage for $|\eta| < 3.3$. The muon momentum resolution is $\sigma(1/p) = 0.18(p-2)/p^2 \oplus 0.008$ with p in GeV/c.

The $W(\ell\nu)\gamma$ candidates were obtained by searching for events containing an isolated lepton with high E_T, large missing transverse energy, $\not\!\!E_T$, and an isolated photon.

The $W(e\nu)\gamma$ sample was selected from events passing a trigger which requires an isolated EM cluster with $E_T > 20$ GeV and $\not\!\!E_T > 20$ GeV. This EM cluster was required to be within the fiducial region of the calorimeter, $|\eta| < 1.1$ and at least 0.01 radians away from the azimuthal boundaries between the 32 EM modules in the central calorimeter (CC), or within $1.5 < |\eta| < 2.5$ in the end calorimeters (ECs). Kinematic selection was made requiring $E_T^e > 25$ GeV, $\not\!\!E_T > 25$ GeV, and $M_T > 40$ GeV/c^2, where M_T is the transverse mass of the electron and the $\not\!\!E_T$ vector defined by $M_T = [2E_T^e \not\!\!E_T(1-\cos\phi^{e\nu})]^{1/2}$, and $\phi^{e\nu}$ is the azimuthal angle between the electron and the $\not\!\!E_T$ vector. The electron cluster must (i) have a ratio of EM energy to the total shower energy greater than 0.9; (ii) have lateral and longitudinal shower shape consistent with an electron shower [6]; (iii) have the isolation variable of the cluster, I, less than 0.15, where I is defined as $I = (E(0.4) - EM(0.2))/EM(0.2)$, and $E(0.4)$ is the total calorimeter energy inside a cone of radius $\mathcal{R} \equiv \sqrt{(\Delta\eta)^2 + (\Delta\phi)^2} = 0.4$, and $EM(0.2)$ is the EM energy inside a cone of 0.2 in the same units; and (iv) have a matching track in the drift chambers.

The $W(\mu\nu)\gamma$ sample was selected from events passing a trigger requiring an EM cluster

with $E_T > 7$ GeV and a muon track with transverse momentum, p_T, greater than 5 GeV/c. A muon track was required to be in the region of $|\eta| < 1.7$. Kinematic selection was made requiring $p_T^\mu > 15$ GeV/c and $\not\!\!E_T > 15$ GeV. The muon track must (i) have hits in the inner drift-tube layer; (ii) have a good track fit in the muon system; (iii) traverse a minimum field integral of 2.0 Tm; (iv) have a time within 100 ns of the beam crossing; (v) have an impact parameter, computed using only hits in the muon system, smaller than 22 (15) cm in the bend (non-bend) view; (vi) be isolated from a nearby jet in η–ϕ space, $\Delta R_{\mu-\mathrm{jet}} > 0.5$; and (vii) have a matching track in the drift chambers as well as a minimum energy deposition of 1 GeV in the calorimeter. To reduce the background due to $Z\gamma$ production, events were rejected if they contained an extra muon track with $p_T^\mu > 8$ GeV.

The requirements on photons were common to both the $W(e\nu)\gamma$ and the $W(\mu\nu)\gamma$ samples. We required $E_T^\gamma > 10$ GeV and the same geometrical and quality selection as for electrons, except that we required a tighter isolation, $I < 0.10$, and that there be no track matching the calorimeter cluster. In addition, we required that the separation between a photon and a lepton be $\mathcal{R}_{\ell\gamma} > 0.7$. This requirement suppresses the contribution of the radiative W decay process, and minimizes the probability for a photon cluster to merge with a nearby calorimeter cluster associated with an electron or a muon. The above selection criteria yielded 11 $W(e\nu)\gamma$ candidates and 12 $W(\mu\nu)\gamma$ candidates.

The background estimate, summarized in Table I, includes contributions from: $W+$jets, where a jet is misidentified as a photon; $Z\gamma$, where the Z decays to $\ell^+\ell^-$, and one of the leptons is undetected or is mismeasured by the detector and contributes to $\not\!\!E_T$; $W\gamma$ with $W \to \tau\nu$ followed by $\tau \to \ell\nu\bar{\nu}$. We estimated the $W+$ jets background using the probability, $\mathcal{P}(j \to \text{“}\gamma\text{”})$, for a jet to be misidentified as a photon determined as a function of E_T of the jet by measuring the fraction of jets in a sample of multijet events that pass our photon identification requirements. The contribution from direct photon events in the multijet sample to $\mathcal{P}(j \to \text{“}\gamma\text{”})$ was subtracted using a conversion method [7]. We found the misidentification probability to be $\mathcal{P}(j \to \text{“}\gamma\text{”}) \sim 4 \times 10^{-4}$ ($\sim 6 \times 10^{-4}$) in the CC (EC) in the E_T region between 10 and 40 GeV, where our photon candidates occur. By

applying $\mathcal{P}(j \to \text{“}\gamma\text{”})$ to the observed E_T spectrum of jets in the inclusive $W(\ell\nu)$ sample, we calculated the total number of $W+$jets background events to be 1.7 ± 0.9 and 1.3 ± 0.7 for $W(e\nu)\gamma$ and $W(\mu\nu)\gamma$, respectively, where the uncertainty is dominated by the uncertainty in $\mathcal{P}(j \to \text{“}\gamma\text{”})$ due to the direct photon subtraction. We tested for a bias in the $W+$jets background estimate due to a possible difference in jet fragmentation (e.g. the number of π^0s in a jet) between jets in the W sample and those in the multijet sample by parameterizing $\mathcal{P}(j \to \text{“}\gamma\text{”})$ further as a function of the EM energy fraction of the jet and found no evidence for a bias. Because the $W+$jets background is computed using observed $W(\ell\nu)$ events, it includes the background originating from ℓ+jets, where ℓ is a jet misidentified as an electron, a cosmic ray muon or a fake muon track.

The backgrounds due to $Z\gamma$ and $W \to \tau\nu$ were estimated using the $Z\gamma$ event generator of Baur and Berger [8] and the ISAJET program [9], respectively, followed by a full detector simulation using the GEANT program [10]. Subtracting the estimated backgrounds from the observed number of events, we found the number of signal events to be

$$N_{\rm sig}^{W(e\nu)\gamma} = 9.0^{+4.2}_{-3.1} \pm 0.9, \quad N_{\rm sig}^{W(\mu\nu)\gamma} = 7.6^{+4.4}_{-3.2} \pm 1.1,$$

where the first uncertainty is statistical, calculated following the prescription for Poisson processes with background given in Ref. [11], and the second is systematic.

The trigger and offline lepton selection efficiencies, shown in Table II, were estimated using $Z \to \ell\bar{\ell}$ and $W \to \ell\nu$ events. The detection efficiency for photons with $E_T > 25$ GeV was determined using electrons from Z decays. For photons with lower E_T there is a decrease in detection efficiency due to the cluster shape requirement, which was determined using test beam electrons, as well as the isolation requirement, which was determined by measuring the energy in a cone of radius $\mathcal{R} = 0.4$ randomly placed in the inclusive $W(e\nu)$ sample. Combining this E_T–dependent efficiency with the probabilities of losing a photon due to e^+e^- pair conversions, 0.10 (0.26) in the CC (EC), and due to an overlap with a random track in the event, 0.065 (0.155), we estimated that the overall photon selection efficiency is 0.43 ± 0.04 (0.38 ± 0.03) at $E_T^\gamma = 10$ GeV, and that it increases to 0.74 ± 0.07

(0.58 ± 0.05) for $E_T^\gamma > 25$ GeV.

We calculated the kinematic and geometrical acceptance as a function of coupling parameters using the Monte Carlo program of Baur and Zeppenfeld [12], in which the $W\gamma$ production and radiative decay processes are generated to leading order, and higher order QCD effects are approximated by a K-factor of 1.335. We used the MRSD_$'$ structure functions [13] and simulated the p_T distribution of the $W\gamma$ system using the observed p_T spectrum of the W in the inclusive $W(e\nu)$ sample. Using the acceptance for SM couplings of 0.11 ± 0.01 for $W(e\nu)\gamma$ and 0.29 ± 0.02 for $W(\mu\nu)\gamma$ and the efficiencies quoted above, we calculated the $W\gamma$ cross section (for photons with $E_T^\gamma > 10$ GeV and $\mathcal{R}_{\ell\gamma} > 0.7$) from a combined $e + \mu$ sample: $\sigma(W\gamma) = 138^{+51}_{-38}(stat) \pm 21(syst)$ pb, where the systematic uncertainty includes the uncertainty (11%) in the $e/\mu/\gamma$ efficiencies, the uncertainty (9.1%) in the choice of the structure functions, the Q^2 scale at which the structure functions are evaluated and the p_T distribution of the $W\gamma$ system, and the uncertainty (5.4%) in the integrated luminosity calculation. The observed cross section agrees with the SM prediction of $\sigma_{W\gamma}^{SM} = 112 \pm 10$ pb within errors. Figure 1 shows the data and the SM prediction plus the background in the distributions of E_T^γ, $\mathcal{R}_{\ell}\gamma$, and the cluster transverse mass defined by $M_T(\gamma\ell;\nu) = (((m_{\gamma\ell}^2 + |\mathbf{E_T^\gamma} + \mathbf{E_T^\ell}|^2)^{\frac{1}{2}} + \not{E}_T)^2 - |\mathbf{E_T^\gamma} + \mathbf{E_T^\ell} + \not{\mathbf{E}}_\mathbf{T}|^2)^{\frac{1}{2}}$. Of the 23 events we observed, 11 events having $M_T(\gamma\ell;\nu) \leq M_W$ are primarily the radiative W decay events plus background.

To set limits on the anomalous coupling parameters, a binned maximum likelihood fit was performed on the E_T^γ spectrum for each of the $W(e\nu)\gamma$ and $W(\mu\nu)\gamma$ samples, by calculating the probability for the sum of the Monte Carlo prediction and the background to fluctuate to the observed number of events. The uncertainties in background estimate, efficiencies, acceptance and integrated luminosity were convoluted in the likelihood function with Gaussian distributions. A dipole form factor with a form factor scale $\Lambda = 1.5$ TeV was used in the Monte Carlo event generation. The limit contours for the CP–conserving anomalous coupling parameters $\Delta\kappa$ and λ are shown in Fig. 2, assuming that the CP–violating anomalous coupling parameters $\tilde{\kappa}$ and $\tilde{\lambda}$ are zero. We obtained limits at the 95% confidence

level (CL) of

$$-1.6 < \Delta\kappa < 1.8\ (\lambda = 0), \quad -0.6 < \lambda < 0.6\ (\Delta\kappa = 0)$$

for $\hat{s} = 0$ (i.e. the static limit). The $U(1)_{EM}$–only coupling of the W boson to a photon, which leads to $\kappa = 0$ ($\Delta\kappa = -1$) and $\lambda = 0$, and thereby, $\mu_W = e/2m_W$ and $Q_W^e = 0$ [14], is excluded at the 80% CL, while the zero magnetic moment ($\mu_W = 0$) is excluded at the 95% CL. Similarly, limits on CP–violating coupling parameters were obtained as $-1.7 < \tilde{\kappa} < 1.7$ ($\tilde{\lambda} = 0$) and $-0.6 < \tilde{\lambda} < 0.6$ ($\tilde{\kappa} = 0$) at the 95% CL. We studied the form factor scale dependence of the results and found that the limits are insensitive to the form factor for $\Lambda > 200$ GeV and are well within the constraints imposed by the S-matrix unitarity [15] for $\Lambda = 1.5$ TeV. We also performed a two dimensional fit including $\mathcal{R}_{\ell\gamma}$, and found that the results are within 3% of those obtained from a fit to the E_T^γ spectrum only. Our results represent the currently most stringent direct limits on anomalous $WW\gamma$ couplings [16], [17].

We thank U. Baur and D. Zeppenfeld for providing us with the $W\gamma$ Monte Carlo program and for many helpful discussions. We thank the Fermilab Accelerator, Computing, and Research Divisions, and the support staffs at the collaborating institutions for their contributions to the success of this work. We also acknowledge the support of the U.S. Department of Energy, the U.S. National Science Foundation, the Commissariat à L'Energie Atomique in France, the Ministry for Atomic Energy and the Ministry of Science and Technology Policy in Russia, CNPq in Brazil, the Departments of Atomic Energy and Science and Education in India, Colciencias in Colombia, CONACyT in Mexico, the Ministry of Education, Research Foundation and KOSEF in Korea and the A.P. Sloan Foundation.

REFERENCES

* Visitor from IHEP, Beijing, China.

‡ Visitor from CONICET, Argentina.

§ Visitor from Universidad de Buenos Aires, Argentina.

¶ Visitor from Univ. San Francisco de Quito, Ecuador.

[1] K. Hagiwara, R.D. Peccei, D. Zeppenfeld and K. Hikasa, Nucl. Phys. **B282**, 253 (1987).

[2] K. Kim and Y-S. Tsai, Phys. Rev. D **7**, 3710 (1973).

[3] U. Baur and E.L. Berger, Phys. Rev. D **41**, 1476 (1990).

[4] DØ Collaboration, S. Abachi *et al.*, Nucl. Instrum. Methods **A338**, 185 (1994).

[5] DØ Collaboration, S. Abachi *et al.*, Nucl. Instrum. Methods **A324**, 53 (1993); DØ Collaboration, H. Aihara *et al.*, Nucl. Instrum. Methods **A325**, 393 (1993).

[6] DØ Collaboration, M. Narain, "Proceedings of the American Physical Society Division of Particles and Fields Meeting," Fermilab (1992), eds. R. Raja and J. Yoh, Vol.2, 1678; R. Engelmann *et al.*, Nucl. Instrum. Methods **A216**, 45 (1983).

[7] DØ Collaboration, S. Fahey, to appear in "Proceedings of the American Physical Society Division of Particles and Fields Meeting," Albuquerque (1994), ed. S. Seidel.

[8] U. Baur and E.L. Berger, Phys. Rev. D **47**, 4889 (1993).

[9] F. Paige and S. Protopopescu, BNL Report BNL38034, 1986 (unpublished), release V6.49.

[10] F. Carminati *et al.*,"GEANT Users Guide," CERN Program Library, December 1991 (unpublished).

[11] Review of Particle Properties, Phys. Rev. D **50**, 1994. Sec.17.5.4.; O. Helene, Nucl.

Instrum. Methods **212**, 319 (1983).

[12] U. Baur, private communication. U. Baur and D. Zeppenfeld, Nucl. Phys. **B308**, 127 (1988).

[13] A.D. Martin, R.G. Roberts and W.J. Stirling, Phys. Rev. D **47**, 867 (1993).

[14] T.D. Lee, Phys. Rev. **140**, 967 (1965).

[15] U. Baur and D. Zeppenfeld, Phys. Lett. **B201**, 383 (1988).

[16] UA2 Collaboration, J. Alitti *et al.*, Phys. Lett. **B277**, 194 (1992).

[17] CDF Collaboration, F. Abe *et al.*, Phys. Rev. Lett. **74**, 1936 (1995).

TABLES

TABLE I. Summary of $W(e\nu)\gamma$ and $W(\mu\nu)\gamma$ data and backgrounds.

	$W(e\nu)\gamma$	$W(\mu\nu)\gamma$
Source:		
$W+$jets	1.7 ± 0.9	1.3 ± 0.7
$Z\gamma$	0.11 ± 0.02	2.7 ± 0.8
$W(\tau\nu)\gamma$	0.17 ± 0.02	0.4 ± 0.1
Total Background	2.0 ± 0.9	4.4 ± 1.1
Data	11	12

TABLE II. Summary of trigger (ϵ_{trig}) and lepton selection (ϵ_ℓ) efficiencies.

	$W(e\nu)\gamma$		$W(\mu\nu)\gamma$	
	$\lvert\eta\rvert < 1.1$	$1.5 < \lvert\eta\rvert < 2.5$	$\lvert\eta\rvert < 1.0$	$1.0 < \lvert\eta\rvert < 1.7$
ϵ_{trig}	0.98 ± 0.02	0.98 ± 0.02	0.74 ± 0.06	0.35 ± 0.14
ϵ_ℓ	0.79 ± 0.02	0.78 ± 0.03	0.54 ± 0.04	0.22 ± 0.07

FIGURES

FIG. 1. Distribution of (a) E_T^γ, (b) $\mathcal{R}_{\ell\gamma}$ and (c) $M_T(\gamma\ell;\nu)$ for the $W(e\nu)\gamma + W(\mu\nu)\gamma$ combined sample. The points are data. The shaded areas represent the estimated background, and the solid histograms are the expected signal from the Standard Model plus the estimated background.

FIG. 2. Limits on (a) CP–conserving anomalous coupling parameters $\Delta\kappa$ and λ, and on (b) the magnetic dipole, μ_W, and electric quadrupole, Q_W^e, moments. The ellipses represent the 68% and 95% CL exclusion contours. The symbol, $\bullet$, represents the Standard Model values, while the symbol, $\star$, indicates the $U(1)_{EM}$–only coupling of the W boson to a photon, $\Delta\kappa = -1$ and $\lambda = 0$ ($\mu_W = e/2m_W$ and $Q_W^e = 0$).

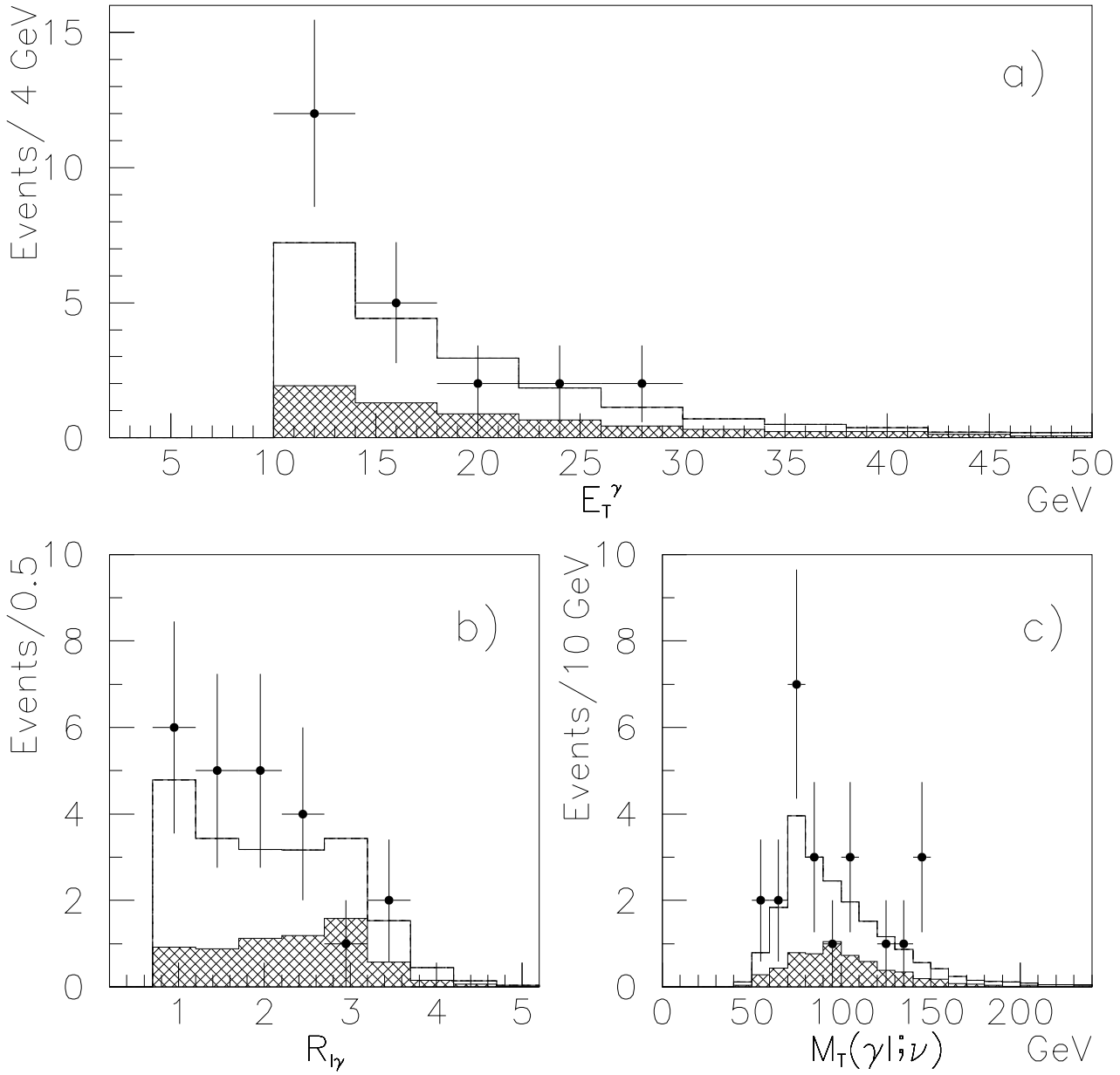

FIG. 1. Distribution of (a) E_T^γ, (b) $\mathcal{R}_{\ell\gamma}$ and (c) $M_T(\gamma\ell;\nu)$ for the $W(e\nu)\gamma + W(\mu\nu)\gamma$ combined sample. The points are data. The shaded areas represent the estimated background, and the solid histograms are the expected signal from the Standard Model plus the estimated background.

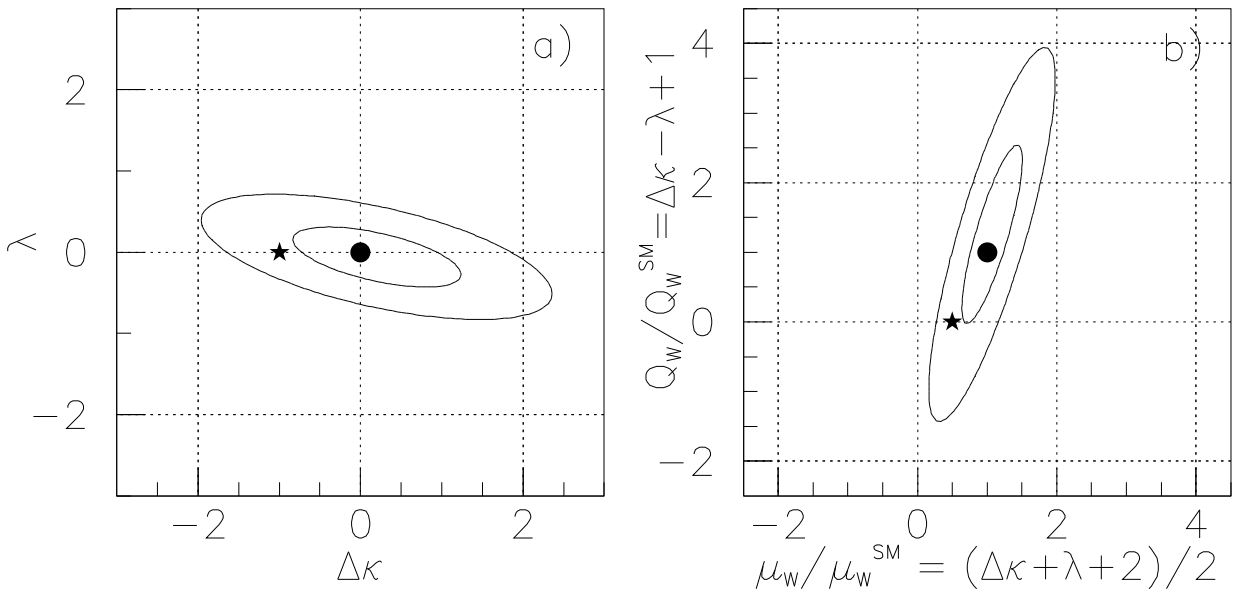

FIG. 2. Limits on (a) CP–conserving anomalous coupling parameters $\Delta\kappa$ and λ, and on (b) the magnetic dipole, μ_W, and electric quadrupole, Q_W^e, moments. The ellipses represent the 68% and 95% CL exclusion contours. The symbol, $\bullet$, represents the Standard Model values, while the symbol, $\star$, indicates the $U(1)_{EM}$–only coupling of the W boson to a photon, $\Delta\kappa = -1$ and $\lambda = 0$ ($\mu_W = e/2m_W$ and $Q_W^e = 0$).